Chemical Physics Letters 506 (2011) 42–45

Contents lists available at ScienceDirect

Chemical Physics Letters

journal homepage: www.elsevier.com/locate/cplett

Electronic hole localization in rutile and anatase TiO_2 – Self-interaction correction in Δ-SCF DFT

Paweł Zawadzki *, Karsten Wedel Jacobsen, Jan Rossmeisl

Department of Physics, Center for Atomic-Scale Materials Design, Technical University of Denmark, DK-2800 Kgs. Lyngby, Denmark

ARTICLE INFO

Article history:
Received 30 November 2010
In final form 2 March 2011
Available online 4 March 2011

ABSTRACT

We study electronic hole localization in rutile and anatase titanium dioxide by means of Δ-Self-Consistent Field Density Functional Theory. In order to compare stabilities of the localized and the delocalized hole states we introduce a simple correction to the wrong description of the localization processes within DFT. The correction removes the non-linearity of energy for fractional excitations. We show that the self-trapped and the delocalized hole states have comparable stability in rutile TiO_2 whereas in anatase the former is favoured. The theoretical prediction of the adiabatic Potential Energy Surfaces for the hole localization compares well with published photoluminescence measurements.

1. Introduction

Density Functional Theory (DFT) with the (semi-)local Density Functional Approximation (DFA) is an inexpensive computational method for a wide spectrum of electronic structure problems. However, the introduced approximations turn out to be too crude for certain problems. One of these is the description of localized states in extended systems where spurious electron self-interaction leads to an over-delocalization of electronic states. The evident symptom of this tendency is the wrong curvature of the energy for fractional electron systems. GGAs are δN-convex thus they favor fractional, delocalized states [1,2]. This bias is especially apparent in the failure to predict relative stabilities of free and (self-)trapped charges [3].

An example process where charge trapping is of great technological importance is photo-catalysis on TiO_2 surfaces [4]. TiO_2 is utilized in processes such as water and air purification and is of potential use as a catalyst for solar into chemical energy conversion [4–6]. Oxidative power for those processes is delivered through trapped hole states generated in photoexcited TiO_2. Although a lot of research has been done, the exact nature of the hole traps in TiO_2 remains unclear. Measurements such as electron paramagnetic resonance [7,8], photoluminescence [9–11], transient absorption [12,13] spectroscopies or oxygen photodesorption [14] show that hole trapping sites in rutile and anatase TiO_2 are centered on oxygen atoms, and that both surface and lattice sites are present. However, the two phases differ in photo-catalytic activity and the precise reason for this is not clear [4]. Certainly, a different charge trapping capability of the two phases [15] is of vital importance here as the energetics of trapping sites in the bulk and in the surface layers will determine holes availability for the reaction and their oxidative power.

In this Letter, we consider hole trapping in the bulk of photoexcited TiO_2 by means of the Δ-Self-Consistent Field (Δ-SCF) DFT [16]. We introduce a simple procedure which is parameter free and provides a systematic way to search for trapping sites in extended systems. To estimate relative stabilities of localized versus delocalized states we correct DFT energies for the biased description of charge localization processes. We associate this correction with the non-linearity of the energy for fractional excitations and apply the procedure to rutile and anatase TiO_2. We find that the electronic hole localizes on a lattice oxygen forming a small-polaron [17–19] trapping center in agreement with experimental measurements [20] and LDA + U calculations [21]. Our work provides relative stabilities of the delocalized and the localized hole states and compares them with photoluminescence data.

2. Computational details

We performed DFT calculations within the Projector-Augmented Wave formalism implemented in the GPAW code [22,23]. Pseudo wave-functions/densities and potentials were represented on an uniform, real-space grid with a spacing of 0.2 Å. To account for exchange–correlation effects we used the RPBE functional [24].

Excited-state (ES) energies were obtained with generalized Δ-SCF [25,16]. Application of the more rigorous, but computationally much more demanding, ES methodologies is not feasible since the localized nature of the trapped hole state involves long-range atomic relaxations which can only be captured in large systems.

The TiO_2 rutile ($P4_2/mnm$) and anatase ($I4_1/amd$) atomic structures were optimized, and the resulting cell parameters (rutile: $a = 4.691$, $c = 2.975$, $u = 0.3061$; anatase: $a = 3.829$, $c = 9.744$,

* Corresponding author. Fax: +45 4593 2399.
E-mail address: zawpaw@fysik.dtu.dk (P. Zawadzki).

0009-2614/$ - see front matter © 2011 Elsevier B.V. All rights reserved.
doi:10.1016/j.cplett.2011.03.001

$u = 0.2062$) differed by less than 3% from the experimental ones [5,26]. We have studied a range of unit cell sizes defined by lattice vectors $\mathbf{a}' = m(\mathbf{a} + \mathbf{b})$, $\mathbf{b}' = n(\mathbf{a} - \mathbf{b})$, $\mathbf{c}' = o\mathbf{c}$ for rutile; and $\mathbf{a}' = p\mathbf{a}$, $\mathbf{b}' = q\mathbf{b}$, $\mathbf{c}' = r\mathbf{c}$ for anatase, $\mathbf{a}$, $\mathbf{b}$ and $\mathbf{c}$ being the vectors of the respective tetragonal crystallographic cells. For rutile $[m,n,o] = [3,2,2]$ and for anatase $[p,q,r] = [2,3,2]$ cells were found sufficient to describe localization phenomena, both containing 144 atoms. The Brillouin zone was sampled on $3 \times 2 \times 2$ and $3 \times 2 \times 1$ Monhorst–Pack mesh for rutile and anatase, respectively.

3. Procedure

Application of (semi-) local DFA to polaronic systems is often troublesome. Classic example of their failure is hole localization around aluminum substitution in α-quartz. GGA predict the hole to be delocalized over four oxygen atoms surrounding the defect [27] whereas experiments clearly indicate that the hole is mostly confined to one oxygen.

The problem of charge self-trapping is even more difficult as the delocalization error takes its maximum – we compare a completely delocalized state with a fully localized one. Therefore a simple use of (semi)-local DFA does not provide localized solution for the electronic hole in TiO_2. Here we approach the problem by making an assumption on the nature of localized hole state and then we estimate its stability in a possibly unbiased way. The procedure consist of four steps: we (1) produce an initial hole orbital; (2) find a distortion associated with the presence of a hole orbital in the Valence Band (VB); (3) construct the Potential Energy Surface (PES) along the distortion; (4) correct PES for the over-delocalization error.

3.1. Initial guess

A reasonable choice for a trial hole orbital can be derived from the Projected Density of States (PDOS) (Figure 1). Both in rutile and anatase the top of the VB is composted mostly form the oxygen's p orbitals perpendicular to the flat OTi_3 unit, $p_\perp$. Since $p_\perp$ participates in π(Ti–O) bonding which is considerably weaker than σ(Ti–O) it forms the top of the VB and offers less destabilization upon electron removal. Choice of a single $p_\perp$ is also supported through a group theoretical reasoning: $p_\perp$ is the only oxygen's atomic orbital belonging to the b_1 irreducible representation of the local OTi_3 symmetry point group – C_{2v}. Since b_1 is largely non-bonding it is highest in energy. We construct the orbital by taking the difference between the true and the pseudo oxygen atomic $p_\perp$ orbital inside an augmentation sphere of radius 1.4 Bohr, $\phi_{p_\perp}(\mathbf{r}) = [\phi^{O}_{p_\perp}(\mathbf{r} - \mathbf{R}^{O}) - \tilde{\phi}^{O}_{p_\perp}(\mathbf{r} - \mathbf{R}^{O})]$, where $\mathbf{R}^{O}$ is the position of the chosen oxygen atom and $\tilde{\phi}^{O}_{p_\perp}, \phi^{O}_{p_\perp}$ are pseudo partial wave and all-electron partial wave respectively, of the atom [16].

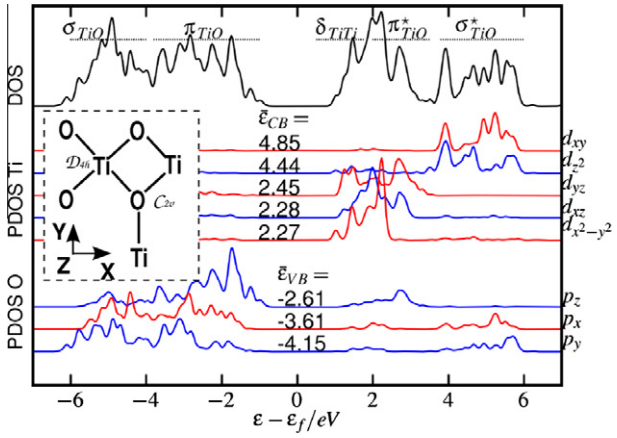

Figure 1. Rutile – PDOS onto O and Ti atomic orbitals. $\hat{\varepsilon}$ denote projections centers. The inset shows the local symmetry around O and Ti atoms. The top of the VB is formed from the oxygen's $p_\perp$ (the p orbital perpendicular to the flat OTi_3 unit, p_z in the inset coordinates) contributing to the π(TiO) bond.

3.2. Finding distortion

To find the distortion associated with the presence of the localized hole orbital, $\phi_{p_\perp}$, in the VB we excite an electron from its normalized expansion in M occupied states to the lowest conduction band. This is achieved by modifying the electron density at each self-consistency cycle,

$$n(\mathbf{r}) = \sum_{i=1}^{M} |\psi_i(\mathbf{r})|^2 - \sum_{i,j=1}^{M} c_i^* c_j \psi_i^*(\mathbf{r})\psi_j(\mathbf{r}) + |\psi_{M+1}(\mathbf{r})|^2, \quad (1)$$

where $c_i = \langle \phi_{p_\perp} | \psi_i \rangle / \left\{ \sum_{j=1}^{M} |\langle \phi_{p_\perp} | \psi_j \rangle|^2 \right\}^{1/2}$. With such constraint density we now relax the atomic structure. Initially the expansion of the hole orbital, $\phi_{p_\perp}(\mathbf{r})$, in Bloch states is largely delocalized over all the equivalent oxygen atoms. However, as the self-consistency cycle and the structure relaxation proceed a single band-gap state localized on the chosen oxygen atom is formed. Hence a rather simple approximation, $\phi_{p_\perp}(\mathbf{r})$, leads to a state having O^- ionic character. The electron removal weakens the π(TiO) bond and results in its elongation. The direction of the distortion around the created localized hole is along the OTi_3 breathing mode.

3.3. Constructing PES

Using linear interpolation between the equilibrium Ground State (GS) geometry and the distorted one we generate set of structures. Along this path we then calculate PES by removing an electron from the top of the Valence Band (VB) and placing it at the bottom of the Conduction Band (CB).

$$n(\mathbf{r}) = \sum_{i}^{M-1} |\psi_i(\mathbf{r})|^2 + |\psi_{M+1}(\mathbf{r})|^2. \quad (2)$$

The frontier bands correspond to VB and CB maximum and minimum, respectively, as large unit cells are used and the band structure is multiply folded. The resulting PES are shown on Figure 2. Clearly, for a larger distortion the ES PES deviates from an ideal

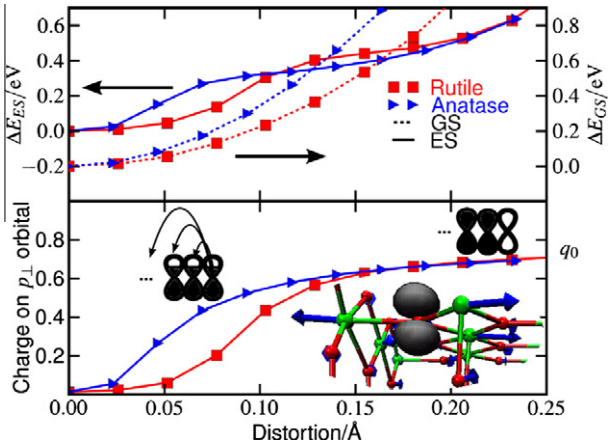

Figure 2. Top: Potential Energy Surfaces for the hole localization on the $p_\perp$ orbital as a function of the distortion along the OTi_3 breathing mode in rutile and anatase. The distortion is an average elongation of the three Ti–O bonds surrounding the trapping center. Bottom: charge localization on the $p_\perp$ orbital. q_0 denotes the maximum contribution of the $p_\perp$ orbital to the hole density. The inset structure shows the direction of the distortion for rutile. Charge localization seems to lead to stabilization of the excited state.

harmonic behavior of the GS PES and the presence of a localized and delocalized states can be distinguished. The hole self-traps on one sites and the degree of localization is monitored with the contribution of $\phi_{p_\perp}(\mathbf{r})$ to the hole density. This contribution increases from $\propto N^{-1}$, N being unit cell size, to about 0.75 (for all cell sizes used) as the structure distorts. The excited electron remains delocalized over all the titanium atoms thus it does not bias the localized or the delocalized nature of the hole through Coulombic interaction. We calculated a non-screened Coulomb interaction between the hole and the excited electron and found a difference of $\approx 0.05 - 0.10$ eV between the localized and the delocalized hole states. The inclusion of screening (optical dielectric constant $\epsilon_\infty \approx 7$ [28]) makes this effect negligible. A proper description of titanium d states might lead to electron self-trapping [29] but it is not an issue here.

3.4. Correcting PES

States along the calculated PES are characterized by different degree of localization. At the non-distorted structure the hole is delocalized over all the oxygen lattice sites, the degree of the hole localization is $1/N$ where N is the number of oxygen lattice sites. As we move along the distorting coordinate the hole localizes on one site therefore the degree of localization tends to 1. δN-convexity of (semi-) local DFA energetically favors charge delocalization therefore areas on PES due to more localized states are erroneously elevated. To correct for this inconsistent description we employ the fact that the exact DFT energy is linear with a change in the occupation of the Highest Occupied State (HOS) [30]. The more localized the HOS is the larger is its nonlinear deviation. If HOS is completely delocalized (delocalized limit) a straight line behavior is recovered, though with incorrect slope [2].

The ES energy is generally not linear in fractional excitation number. However, at low intensity excitation when one of the excited carries remains delocalized over large unit cell the electron–hole interaction is small and more importantly constant along the distortion. The latter is in analogy to the interaction of a charge with uniformly charged background. Therefore only a residual, fixed nonlinearly will be added to a larger effect due to charge localization.

Accordingly, by removing the non-linearity of ES energy at different distortion we achieve a more consistent description – we treat all the points along ES PES at delocalized limit. Assuming that the shape of GS PES is correct along the distortion the ES energy at delocalized limit equals

$$E_{\mathrm{ES}}^{\infty} = E_{\mathrm{ES}} - E_{\mathrm{LC}} = E_{\mathrm{GS}} + \left.\frac{\partial E_{\mathrm{ES}}(\lambda)}{\partial \lambda}\right|_{\lambda=0}, \tag{3}$$

where λ is fractional excitation number and E_{LC} is the sought correction to ES PES.

We calculate the correction to the ES PES at different distortion by constructing, $E_{ES}(\lambda)$ and fitting to a parabola $E_{ES}(\lambda) = a\,\lambda^2 + b\lambda + c$, where a is the sought correction, E_{LC} (Figure 3a).

4. Discussion

On Figure 3b the corrected PESs are presented. In rutile stabilities of the delocalized and the localized hole stats are comparable, whereas in anatase the latter is favoured by 0.2 eV. Energetics of band gap states can be accessed with photoluminescence (PL) measurements. At low temperatures a PL peak of a vibronic transition is centered at the direct (Franck–Condon) transition from the minimum of the ES PES to the GS PES (see the inset in Figure 3b). Neglecting the difference between zero point energies of the GS and the ES the position of the PL peak is given by $P = E_g - R - S$,

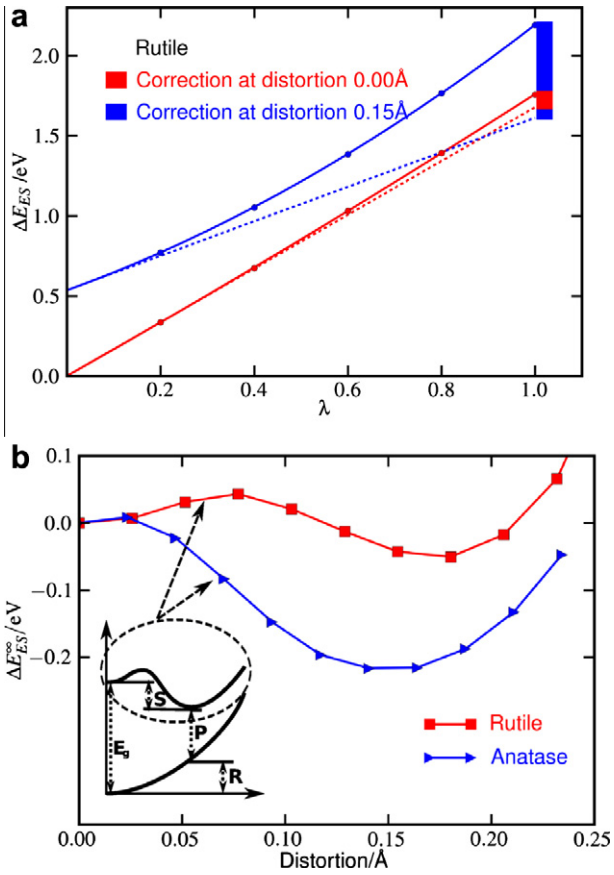

Figure 3. (a) Fractional excitation energy. λ is a fraction of an electron moved from the VB to the CB. The localization error is a non-linearity of the fractional excitation energy taken at one electron excitation ($\lambda = 1$). (b) The corrected PES. The distortion leads to the formation of a small-polaron trapping center. Since the VB edges in rutile and anatase coincide we conclude that anatase offers stronger bulk trapping centers. The inset scheme shows the photoluminescent transition, P, from the minimum of the ES PES. S is the small-polaron stabilization, R is the GS energy associated with the ES PES displacement.

where E_g is the band gap (3.0 eV and 3.2 eV [5] for rutile and anatase, respectively), R is the GS energy associated with the excited state PES displacement and S is the small-polaron stabilization. Accordingly, we locate PL peaks at 2.2 and 2.5 eV for anatase and rutile, respectively. The P value for anatase is smaller that for rutile, despite anatase larger band gap, E_g. The reason for this is both stronger polaron binding and larger energy associated with the distortion, R. The experimental value of the PL transition for anatase, measured picoseconds after excitation, amounts to 2.3 eV and is red-shifted by 0.2 eV within nanoseconds [11]. For rutile only nanosecond data is available and values in the range of 2.6–2.9 eV [9,10] are reported. Sub-nanosecond evolution of the photoluminesence [11], and also of the absorption [13] spectra, is possibly due to redistribution of holes between trapping sites both in the bulk and on the surface. The agreement between the experimental and the calculated values, and more importantly the prediction of a smaller P value for anatase despite a larger band gap, suggests that these transitions are due to the bulk hole small-polaron and the conduction band electron recombinations.

Based on Huang–Rhys model [31] for a single frequency, ω_0, coupled vibronic transition we estimate the band's Full Width at Half Maximum. For Gaussian shaped peak $FWHM = 2\sqrt{2\ln(2)R\hbar\omega_o}$, what gives 0.5 and 0.7 eV using $\hbar\omega_o$ values of the high frequency longitudinal optic mode of 0.10 eV [32] and 0.11 eV [33] for rutile and anatase, respectively. Calculated widths agree with the observed broadness of the PL peaks.

The positions of the valence band edges with respect to the vacuum level coincide in rutile and anatase TiO_2 [4]. This allows us to directly compare stabilities of the localized hole states in both phases. Clearly anatase offers stronger bulk trapping centers.

5. Conclusion

In conclusion, our simple procedure provides a systematic way to search for trapping sites in extended systems. Application of Δ-SCF allows to probe a system with a desired density perturbation. To estimate stabilities of the found trapping sites we use a simple correction based on the non-linearity of the energy versus the fractional electron number. In this respect the procedure resembles DFT + U which for a certain parameter U removes the incorrect curvature of energy as a function of number of electrons [34]. However, DFT + U also affects eigenvalues, here we only remove the biased description of localization process. Our procedure is simple and parameter free. By far the largest material-specific variable is a choice of an initial orbital. A more thorough discussion will be published in future.

Using the described methodology we have shown that the stability of the delocalized and the self-trapped polaron hole states in rutile TiO_2 bulk is comparable, whereas in anatase the trapped hole state is favoured by 0.2 eV. Our results are in good agreement with the published photoluminesence spectra and provide a compelling argument favouring small-polaron as the searched hole trapping center in TiO_2.

Acknowledgments

CAMD is funded by the Lundbeck foundation. The Catalysis for Sustainable Energy initiative is funded by the Danish Ministry of Science, Technology and Innovation. This work was supported by the Danish Center for Scientific Computing. Support from the Danish Council for Technology and Innovation's FTP program and the Danish Council for Strategic Research though the HyCycle Center (No. 2104-07-0041) is acknowledged.

References

[1] P. Mori-Sanchez, A.J. Cohen, W. Yang, Phys. Rev. Lett. 102 (6) (2009) 066403.
[2] P. Mori-Sanchez, A.J. Cohen, W. Yang, Phys. Rev. Lett. 100 (14) (2008) 146401.
[3] J.L. Gavartin, P.V. Sushko, A.L. Shluger, Phys. Rev. B 67 (3) (2003) 035108.
[4] A. Fujishima, X. Zhang, D.A. Tryk, Surf. Sci. Rep. 63 (12) (2008) 515.
[5] U. Diebold, Surf. Sci. Rep. 48 (5-8) (2003) 53.
[6] A. Valdes, G.-J. Kroes, J. Phys. Chem. C 114 (3) (2010) 1701.
[7] O.I. Micic, Y.N. Zhang, K.R. Cromack, A.D. Trifunac, M. Thurnauer, J. Phys. Chem. 97 (28) (1993) 7277.
[8] R.F. Howe, M. Gratzel, J. Phys. Chem. 91 (14) (1987) 3906.
[9] K. Fujihara, S. Izumi, T. Ohno, M. Matsumura, J. Photochem. Photobiol. B 132 (1) (2000) 99.
[10] N. Harada, M. Goto, K. Iijima, H. Sakama, N. Ichikawa, H. Kunugita, K. Ema, Jpn. J. Appl. Phys. 1 46 (7A) (2007) 4170.
[11] L. Cavigli, F. Bogani, A. Vinattieri, V. Faso, G. Baldi, J. Appl. Phys. 106 (5) (2009) 053516.
[12] T. Yoshihara et al., J. Phys. Chem. B 108 (12) (2004) 3817.
[13] Y. Tamaki, A. Furube, M. Murai, K. Hara, R. Katoh, M. Tachiya, Phys. Chem. Chem. Phys. 9 (12) (2007) 1453.
[14] T.L. Thompson, J.T. Yates, J. Phys. Chem. B 109 (39) (2005) 18230.
[15] H. Tang, F. Levy, H. Berger, P.E. Schmid, Phys. Rev. B 52 (11) (1995) 7771.
[16] J. Gavnholt, T. Olsen, M. Engelund, J. Schiotz, Phys. Rev. B 78 (7) (2008) 075441.
[17] A.M. Stoneham et al., J. Phys.: Condens. Matter 19 (25) (2007) 255208.
[18] O.F. Schirmer, J. Phys.: Condens. Matter 18 (43) (2006) R667.
[19] A.L. Shluger, A.M. Stoneham, J. Phys.: Condens. Matter 5 (19) (1993) 3049.
[20] S. Yang, A.T. Brant, L.E. Halliburton, Phys. Rev. B 82 (3) (2010) 035209.
[21] N.A. Deskins, M. Dupuis, J. Phys. Chem. C 113 (1) (2009) 346.
[22] J.J. Mortensen, L.B. Hansen, K.W. Jacobsen, Phys. Rev. B 71 (3) (2005) 035109.
[23] J. Enkovaara et al., J. Phys.: Condens. Matter 22 (25) (2010) 253202.
[24] B. Hammer, L.B. Hansen, J.K. Norskov, Phys. Rev. B 59 (11) (1999) 7413.
[25] R.O. Jones, O. Gunnarsson, Rev. Mod. Phys. 61 (3) (1989) 689.
[26] J.I. Martinez, H.A. Hansen, J. Rossmeisl, J.K. Norskov, Phys. Rev. B 79 (4) (2009) 045120.
[27] J. Laegsgaard, K. Stokbro, Rev. Lett. 86 (53) (2001) 2834.
[28] G.M. Rignanese, X. Rocquefelte, X. Gonze, A. Pasquarello, Int. J. Quant. Chem. 101 (6) (2005) 793.
[29] E. Finazzi, C. Di Valentin, G. Pacchioni, A. Selloni, J. Chem. Phys. 129 (15) (2008) 154113.
[30] J.F. Janak, Phys. Rev. B 18 (12) (1978) 7165.
[31] A.M. Stoneham, Theory of Defects in Solids, Oxford University Press, 1975.
[32] J.G. Trayler, H.G. Smith, R.M. Nicklow, M.K. Wilkinson, Phys. Rev. B 3 (10) (1971) 3457.
[33] R.J. Gonzalez, R. Zallen, H. Berger, Phys. Rev. B 55 (11) (1997) 7014.
[34] M. Cococcioni, S. de Gironcoli, Phys. Rev. B 71 (3) (2005) 035105.